

# Insert Dome Gradient Coils for Brain Imaging

J. Leggett<sup>1</sup>, D. Green<sup>1</sup>, R. Bowtell<sup>1</sup>

<sup>1</sup>Sir Peter Mansfield Magnetic Resonance Centre, School of Physics and Astronomy, University of Nottingham, Nottingham, United Kingdom

## Introduction

Insert gradient coils offer significant advantages for brain imaging as a result of the large increase in gradient performance that is achieved as the coil size is reduced. It has been shown previously that head-sized hemispherical gradient coils offer further improvements in performance compared with cylindrical insert coils [1], allowing very large gradients to be generated with short rise-times. However the enhanced performance is compromised when torque-balancing is incorporated into the design of transverse hemispherical coils. Here, we show how the addition of a short, cylindrical coil section to the open end of the hemisphere, overcomes this problem, allowing the design of torque-balanced gradient coils suitable for brain imaging, which have significantly higher efficiency at fixed inductance than conventional cylindrical insert coils. Using this approach, a full three-axis, dome gradient coil set has been designed, built and subsequently used in brain imaging experiments at 3 T.

## Theory

Methods have previously been presented for the separate design of cylindrical [2,3] and hemispherical [1] gradient coils. These often involve describing the current distribution in terms of a weighted set of basis functions, whose form is dictated by the coil geometry. Optimal weightings of the basis functions can be identified via minimisation of an appropriate functional [4,5]. Here, each coil is made up of hemispherical and cylindrical parts and axially-varying Fourier harmonics have been used in the cylindrical portion of the coil, whilst spherical harmonics were employed for the hemispherical surface. The functional which was minimised was made up of a weighted sum of terms representing the coil's power dissipation, inductance, torque and mean square deviation of the field from a pure gradient over a specified set of points within the ROU [1-7]. Most of these terms are simply made up of the summed contributions from the hemispherical and cylindrical portions of the coil, which can be evaluated using previously described expressions. However, in considering the inductance it is necessary to evaluate the mutual inductance,  $M$ , between the two coil parts. We have therefore derived new expressions for  $M$  by evaluating the integral of the scalar product of the vector potential and current density over the coil surface. Here we only quote the expression for a transverse coil carrying current,  $I$ , which takes the form

$$M_x = -\frac{\mu_0 2\pi}{I^2} \int_{-l}^l dz \sum_{n=1}^N \left( \lambda_n \sin(n\pi z/l) + \zeta_n \cos\left(n - \frac{1}{2}\right)\pi z/l \right) \times \sum_{p=1}^{\infty} \sum_{s=1}^S c_s \gamma_{s,p} \left( \frac{a}{r} \right)^{p+1} \left[ \frac{p \cos\theta P_{p0}(\cos\theta)}{r/a} + \frac{P_{p1}(\cos\theta)}{p(p+1)} (2-p-p^2 \sin^2\theta) \right] \quad (1)$$

where the coil has radius  $a$ , and the cylindrical portion has a total length  $2l$ . The weightings for the  $n^{\text{th}}$  order symmetric and anti-symmetric basis functions of the cylindrical current distribution are  $\zeta$  and  $\lambda$  respectively. The current distribution on the hemisphere is made up of  $S$  spherical harmonics weighted by the coefficients,  $c_s$ , and which are only non-zero on the half-sphere. These are decomposed into a series of full-sphere, spherical harmonics via weightings,  $\gamma_{s,p}$  [1] ( $P_{pm}(\cos\theta)$  is the associated Legendre polynomial of degree,  $p$  and order  $m$ ) and the integral is carried out over the cylindrical coil surface where  $r^2 = (z+l)^2 + a^2$  and  $\sin\theta = a/r$ . The values of the coefficients,  $\zeta$ ,  $\lambda$  and  $c_s$ , which minimise the functional are found by solving a simple set of simultaneous equations generated via differentiation of the functional with respect to each coefficient. Adjustment of the relative weights of the various terms making up the functional allows a trade-off to be made between gradient homogeneity, residual torque and coil inductance and power dissipation. The final current density is generated using the optimal coefficient values and contours of the corresponding stream function are then used to define wire-paths for coil fabrication.

## Method

A three-axis, insert dome gradient coil set was designed for use in human brain imaging. The coil dimensions were based around a commercial, dome, RF coil (Nova Medical, Boston, USA) of 16.5 cm external diameter. The windings of the  $x$ ,  $y$  and  $z$  coils, were located at radii of 0.172, 0.184 and 0.195 m, respectively, and the cylindrical extension of the coil was 11.5 cm long. The target ROU, over which the field variation was forced to deviate by less than 5% from linearity, was defined to be an ellipsoid of revolution about the  $z$ -axis. The ellipsoid had major and minor axes of lengths 15.5 and 11.7 cm respectively, and was centred ~19 cm from the open end of the coil. 67 field constraint points were distributed evenly throughout the ROU. The spatial variation of the magnetic field and the coil efficiency were evaluated by applying an elemental Biot-Savart calculation to the wire-paths (Figs. 1a-c), and for the transverse-gradient coils, the net torque experienced per unit current and field strength was also calculated from the wire-paths. Copper wire of 3 mm diameter, was used for coil construction. Each layer was wound and fixed onto the dome surface and then overlaid with fibre-glass and epoxy resin. The resulting coil set was integrated with a home-built 3T scanner and has subsequently been used in a variety of imaging experiments, including EPI-based fMRI. Gradient coil efficiency was measured via imaging phantoms of known structure.

## Results and Discussion

The parameters characterising the performance of the three-axis, dome-shaped head gradient coil-set are shown in Table 1. The measured and calculated values of the efficiency and inductance are in excellent agreement, thus verifying the analytical expressions used in the coil design process. The mutual inductance of the cylindrical and hemispherical coil portions evaluated using Eq. [1] was verified by comparison with the output of FastHenry (FH), an elemental inductance analysis programme (Table 1). As in standard cylindrical gradient coils, the efficiency,  $\eta$  at fixed inductance,  $L$ , increases rapidly as the coil diameter is reduced, and is higher for axial rather than transverse gradient coils. By winding the  $z$ -gradient coil at the largest radius, comparable performance has however been achieved on all three axes. For comparison, similar-sized, insert cylindrical coils have values of  $\eta/L$  that are more than a factor of two smaller [6,8]. The residual torque experienced by the transverse coils in the dome insert is small, and was found to be reduced by a factor of approximately 500 compared with non-torque-balanced coils of the same geometry. The final coil set weighs about 29 kg, and does not exhibit significant movement when carrying currents of order 200 A in a 3 T field. Figure 1d shows an example inversion recovery echo planar image with 2 mm in-plane resolution and a 256 mm FOV. This was acquired in 44 ms, using a switched gradient in the A-P direction of 0.054 Tm<sup>-1</sup> peak amplitude. Modification of the dome gradient coil design approach to allow incorporation of active screening is currently under investigation.

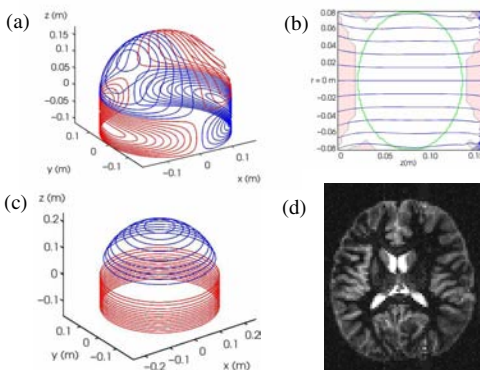


**Figure 1:** Transverse-gradient coil (a) (colour designates sense of current flow) and (b) associated field homogeneity plot, the green line shows the target ROU, while shading indicates where the field variation deviates from linearity by more than 5%; (c) axial-gradient coil; (d) inversion recovery echo planar image (2 x 2 x 4 mm<sup>3</sup> voxel size; TI = 800 ms), acquired using the dome coil set.

	$x$	$y$	$z$
$\eta$ (Theo.) (mTm <sup>-1</sup> A <sup>-1</sup> )	0.34	0.30	0.34
$\eta$ (Meas.) (mTm <sup>-1</sup> A <sup>-1</sup> )	0.34	0.31	0.34
$L$ (Theo.) ( $\mu$ H)	95	76	92
$L$ (Meas.) ( $\mu$ H)	97	76	92
$M_x$ (design) ( $\mu$ H)	4.2	5.4	-3.5
$M_x$ (FH) ( $\mu$ H)	4.7	5.3	-3.9
$\eta^2/L$ (Meas.)	$1.19 \times 10^{-3}$	$1.26 \times 10^{-3}$	$1.26 \times 10^{-3}$
Resistance (Theo.) ( $\Omega$ )	0.059	0.066	0.058
Torque (Theo.) (NmT <sup>-1</sup> A <sup>-1</sup> )	0.0012	0.0024	-

**Table 1.:** Theoretical and measured parameters for the 3-axis dome gradient coil.

## References

- 1) D. Green *et al.*, *Magn. Reson. Med.*, **54** 656-668, (2005).
- 2) R. Bowtell and P. Robyr, *J. Magn. Reson.*, **131** 286-294, (1998).
- 3) J. Leggett *et al.*, *Concepts Magn. Reson. B*, **16** 38-46, (2003).
- 4) J.W. Carlson *et al.*, *Magn. Reson. Med.*, **26** 191-203, (1992).
- 5) R. Turner, *J. Phys. E*, **21** 948-952, (1988).
- 6) D.C Alsop and T.J. Connick, *Magn. Reson. Med.*, **35** 875-886, (1996).
- 7) R. Bowtell and A. Peters, *Magn. Reson. Med.*, **41** 600-608, (1999).